Korean J. Chem. Eng., **31**(2), 179-187 (2014)
DOI: 10.1007/s11814-013-0281-7
pISSN: 0256-1115
eISSN: 1975-7220

REVIEW PAPER

Breakthrough analysis of carbon dioxide adsorption on zeolite synthesized from fly ash

Chang-Han Lee*, Sang-Wook Park, and Seong-Soo Kim*,†**

*Department of Environmental Administration, Catholic University of Pusan, Busan 609-757, Korea
**School of Chemical and Biomolecular Engineering, Pusan National University, Busan 609-735, Korea
(*Received 3 October 2013 • accepted 16 December 2013*)

Abstract−Zeolite (FAZ) was synthesized by the fusion method using coal fly ash to adsorb carbon dioxide. The experimental adsorption was operated batchwise in a laboratory-scale packed-bed adsorber to obtain the breakthrough curves of CO_2 under conditions such as adsorption temperatures (20-80 °C), flow rates of gaseous mixture of carbon dioxide and nitrogen (40-100 cm^3/min), and concentration of CO_2 (3000-10000 ppmv) at atmospheric pressure of 101.3 kPa. The influence of the experimental conditions, such as the gas flow rate, concentration of CO_2 and adsorption temperature on adsorption behavior, was discussed. The deactivation model, combined the adsorption with the deactivation of adsorbent, was used to analyze the physicochemical properties, such as the adsorption kinetics, capacity and heat of adsorption, by fitting the experimental data of the breakthrough curves to this model. The adsorptive activity and capacity of FAZ were as almost same as those of the commercial zeolite of Wako 4A.

Keywords: Adsorption, Carbon Dioxide, Zeolite, Breakthrough Curve, Deactivation Model

INTRODUCTION

Carbon dioxide (CO_2) produced by combustion of fossil fuels is regarded as the most significant greenhouse gas with its increasing accumulation in the atmosphere attracting worldwide attention [1]. Various methods have been used to remove it: absorption by solvent and adsorption by molecular sieve, membrane separation, and cryogenic fractionation. In particular, absorption has been widely used in the chemical industries, as with the Benfield Process [2]. Another technique is dry scrubbing or sorption of CO_2 onto a solid adsorbent. Porous materials such as zeolites and their modified frameworks are seen as promising candidates for carbon capture from post-combustion gas streams because of potential advantages over existing processes such as reduced energy use during regeneration, greater capacity, high selectivity, ease of handling, and fast adsorption kinetics [3].

The kinetic diameters of CO_2 (3.33 Å) and N_2 (3.64 Å) [4] are smaller than the pore aperture of modified zeolites such as cation-exchanged zeolites 3.8 Å [3], aluminosilicate zeolites 4.5 Å [5], natural herschelite-sodium chabozite 4.3 Å [6], chabazite zeolites 3.8 Å [7], zeolites synthesized using coal fly ash 80.9 Å [8], ion-exchanged zeolite beta with alkali 5.5 Å [9], metal organic framework zeolite 13.1 Å [10], activated carbon composite zeolite 28 Å [11], activated alumina based on 13 X typed zeolites 849.4 Å [12], and metal organic framework zeolite 14.1 Å [13], which this allows these adsorbates to diffuse freely. The difference between the polarizability and electric quadrupole moment of CO_2 (4.3×10^{-26} esu·cm^2 and 26.5×10^{-25} cm^3) and those of N_2 (1.52×10^{-26} esu·cm^2 and 17.6×10^{-25} cm^3) affects the selective adsorption of CO_2 from the binary mixture.

Also, the use of a commercial zeolite such as silicate is not cost-effective. The research described below suggests that an alternative adsorption medium (zeolite) may in fact be synthesized on site by a utility from its own fly ash [5,8,15,16]. Substituting zeolite for lime-based scrubbing would reduce transportation and disposal costs of lime and also reduce fly ash disposal to a certain extent [17].

Various contacting devices are available for adsorption systems, such as batch and fixed bed adsorbers. Accurate design of the adsorber is achieved by developing a mass transfer model that adequately describes the kinetics and mechanisms of the adsorption process. A plug-flow heterogeneous surface diffusion model [18] has been developed for representing axial dispersed plug-flow, external mass transfer, adsorption equilibrium on the fluid-particle interface, and intraparticle diffusion for a fixed-bed adsorption column. Analyzing the experimental breakthrough data in a fixed bed is complicated because reasonable diffusivity [19,20] of a solute and physical properties of solid particle need to be known. The conventional isotherm models [18,21] such as the Langmuir, Freundlich, Brunauer-Emmett-Teller, and Dubinin-Radushkevich-Kagener model have been used to obtain the adsorption kinetics, but it is tedious and difficult to prepare the experimental adsorption isotherm. Conversely, the deactivation model (DM) [22-24], as a simplified model, has been used to predict the breakthrough curve, assuming that the formation of a dense product layer over the surface of the adsorbent has caused a drop in the adsorption rate. This model makes the breakthrough curve easily analyzed and correlated with the adsorption isotherm. Park et al. investigated the adsorption kinetics from analysis of the experimental breakthrough data in a fixed bed using DM; adsorption of CO_2 by carbonation of sodium carbonate [25], potassium carbonate [26], and rubidium carbonate [27], adsorption of toluene vapor [28], volatile organic compounds onto granular activated carbon [29], and adsorption of CO_2 onto hybrid MCM41 immobilized by alkyl diamine, such as ethylene diamine [30], propylene diamine [31], butylenes diamine [32]. These studies presented an analysis of the experimental breakthrough data for adsorption of

†To whom correspondence should be addressed.
E-mail: sskim@cup.ac.kr

several gases onto various adsorbent using DM. To our knowledge, no literature report about the adsorption kinetics of CO_2 onto zeolite, synthesized by fly ash, has yet been published except a few articles which have investigated the adsorption capacity of the zeolites by using the conventional isotherm models [5,21-26]. Kopac and Kocabas [33] presented the adsorption kinetics by analyzing the experimental breakthrough data of SO_2 using a commercial adsorbent of molecular sieve 5A samples of Fluka.

In this study, which is one of a series of works [25-32], zeolite was synthesized by the fusion method using coal fly ash to adsorb carbon dioxide, and subsequently used to determine the physicochemical properties, such as the adsorption kinetics, heat of adsorption and adsorption capacity of CO_2 from analysis of the experimental breakthrough data using DM for development of an appropriate adsorbent.

THEORY

The formation of a dense product layer over the solid adsorbent creates an additional diffusion resistance and is expected to cause a drop in the adsorption rate. One would also expect it to cause significant changes in the accessible pore volume, active surface area, and activity per unit area of solid adsorbent with respect to the extent of the adsorption. All of these changes cause a decrease of vacant surface area of the adsorbent with time. In DM, the effects of all of these factors on the diminishing rate of CO_2 capture are combined in a deactivation rate term.

With assumptions [34] of the pseudo-steady state and the isothermal species, the conservation equation of adsorbate in the fixed bed is

$$-Q_o\frac{dC_A}{dS}-k_oC_A\alpha=0 \tag{1}$$

With respect to this equation, axial dispersion in the fixed bed and any mass transfer resistances are assumed to be negligible.

According to the proposed DM, the rate of activity is expressed as

$$-\frac{d\alpha}{dt}=k_dC_A^n\alpha^m \tag{2}$$

The zeroth solution of the deactivation models is obtained by taking n=0, m=1, and the initial activity (α) of adsorbent as unity.

$$\alpha=\exp[-k_o\tau\exp(-k_dt)] \tag{3}$$

Eq. (3) is identical to the breakthrough equation proposed by Suyadal et al. [23] and assumes a fluid phase concentration that is independent of deactivation processes along the adsorber. More realistically, one would expect the deactivation rate to be concentration-dependent and, accordingly, axial-position-dependent in the fixed bed.

To obtain the analytical solution of Eqs. (1) and (2) by taking n=m=1, an iterative procedure is applied. The procedure used here is similar to the paper proposed by Dogu [34] for the approximate solution of nonlinear equations. The zeroth solution of Eq. (3) is substituted into Eq. (2), and the first correction for the activity is obtained by the integration of this equation. Then, the corrected activity expression is substituted into Eq. (1), and integration of this equation gives the first corrected solution for the breakthrough curve.

$$a(t)=\exp\left[\frac{[1-\exp(k_o\tau(1-\exp(-k_dt)))]}{1-\exp(-k_dt)}\exp(-k_dt)\right] \tag{4}$$

This iterative procedure can be repeated for further improvement of the solution. In this procedure, higher-order terms in the series solutions of the integrals are neglected. The breakthrough curve for the deactivation model with two parameters (k_o and k_d) is calculated from the concentration profiles by Eq. (4).

EXPERIMENTAL

1. Synthesis of Zeolite from Fly Ash and its Characteristics

Many patents and technical articles have proposed different hydrothermal activation methods [35-38] to synthesize different zeolites from fly ash, which are based on the dissolution of Al-Si-bearing fly ash phases with alkaline solutions and the subsequent precipitation of zeolitic material. Zeolite (FAZ), used in this study, was synthesized by the fusion method [25] using coal fly ash, obtained from coal combustion processes of a domestic (Hanju Ltd., Korea) company. Previously, the coal fly ash was pretreated at 1073 K for 1 hr in an oven to remove unburned carbon. Then, although $NaAlO_2$ and Na_2CO_3 might be added to the fly ash differently, $NaAlO_2$ 12.3 g and Na_2CO_3 12 g were added to the pretreated fly ash of 10 g to adjust the molar ratio of Si/Al to be 1.5, based on the reference [15], where the zeolite of 4A type was synthesized in the range of 0.9< Si/Al<3.5. And this mixed material was fused in a reactor at 1073 K for 1 hr. The reaction was carried out in an oven with temperature controller under stirred condition. Products were matured at room temperature for 5 hrs and crystallized at 373 K for 5 hrs in deionized water. FAZ, in a powdery form, without using a sieve analyzer was obtained by this final product, which was filtered, washed water and dried at 378 K for 5 hrs. The chemical composition of FAZ was analyzed by XRF (PHILIPS PW2400). The results are shown in Table 1. The surface structure was observed by an SEM (JEOL-6300) and shown in Fig. 1(a). Fig. 1(b) is the image of a commercial zeolite (Wako) of Wako 4A (Wako Chemical Co.). FAZ was similar in the SEM photograph to Wako type. From the particle size distribution curves obtained by a laser diffraction method (HELOS H3078), the volume mean diameter of sample was 23.97 μm. FAZ was used as a powder phase without using a sieve analyzer; its bulk density was

Table 1. Characterization of the synthesized zeolite

Component	Weight [%]
SiO_2	35.61
Al_2O_3	20.07
Na_2O	12.89
CaO	21.39
SO_3	6.18
Fe_2O_3	1.06
MgO	1.14
TiO_2	0.44
etc.	1.22
Total	100.00
Si/Al mole ratio	1.51
Crystallinity (%)	54

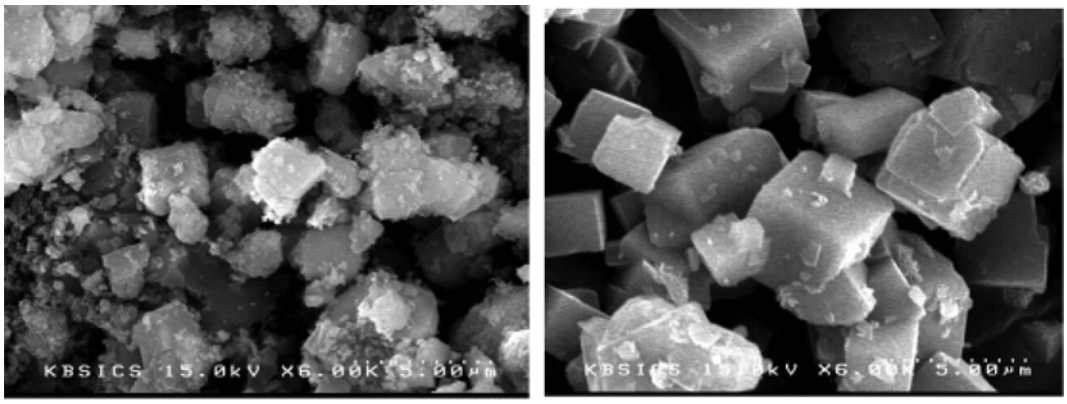

Fig. 1. SEM image patterns of synthesized zeolite (a) and Wako 4A zeolite (b).

measured by a conventional method using a pycnometer, and its value was 867.2 kg/m^3. Specific surface area, total pore volume, and average pore diameter were measured using BET technique (Autosorb-1, Quantachrome Co.), and their values were 122.1 m^2/g, 0.1546 cm^3/g, 5.06 nm, respectively; the values of Wako were 77.74 m^2/g, 0.1329 cm^3/g, and 6.84 nm, respectively. The shape of FAZ was a powder type, and Wako, a bead of 1.4-2.36 mm. The bed porosity of the fixed bed was measured by a conventional method [16] using a mass cylinder and its value was 0.79. The nitrogen gas used as a carrier gas for CO_2 has a purity >99.9%.

2. An Apparatus for CO_2 Adsorption and its Operation

Adsorption of CO_2 (Fig. 2) was carried out in the presence of an adsorbent in a fixed bed of Pyrex glass with internal diameter of 2 cm. CO_2 was carried by N_2. The concentration of CO_2 in the nitrogen stream at the inlet and outlet of the fixed bed was measured by a gas chromatograph, respectively. The flow rate of gas mixture of CO_2 and N_2 was within the range of 40-100 cm^3/min (measured at 25 °C) and the concentration of CO_2 was within the range of 3000-10000 ppmv. The adsorption temperature was in the range of 20-80 °C. The amount of adsorbent was fixed at 2 g. Experiments were repeated three times to obtain the average value for each type of experiment. A gas chromatograph (detector: thermal conductivity detector; column: Haysep D (10 feet by 1/8 inch of stainless steel; detector temperature: 190 °C; feed temperature: 160 °C; flow rate of He: 25.7 cm^3/min; retention time of N_2, CO_2: 1.497, 2.08 min, respectively) was connected to the exit stream of the adsorber allowing for on-line analysis of CO_2 and N_2.

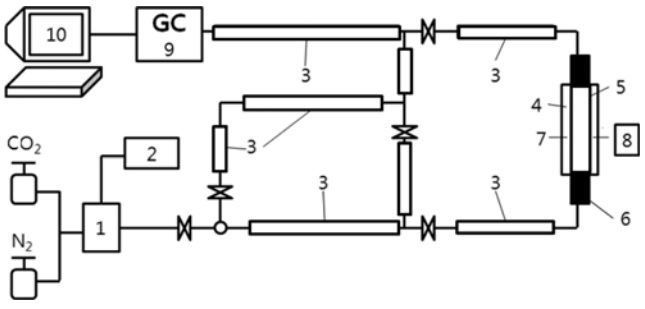

Fig. 2. Schematic diagram of a fixed bed apparatus.

1. Mass flow controller
2. Flow indicator
3. heating line
4. Furnace
5. Sample
6. Glass wool
7. Temperature probe
8. Temperature controller
9. GC (gas chromatography)
10. Personal computer

The adsorbent was supported by glass wool from both ends. The adsorber was placed into a tubular furnace equipped with a temperature controller. Temperature profiles were not observed within this section. All of the flow lines between the adsorber and the gas analyzer were insulated to keep a desired temperature. Three-way valves placed before and after the adsorber allowed for flow of the gaseous mixture through the bypass line during flow rate adjustments. Composition of the inlet stream was checked by the analysis of the stream flowing through the bypass line at the start of experiments. The experimental procedure used to obtain the breakthrough curve of CO_2 was identical to that reported in detail previously [13].

RESULTS AND DISCUSSION

To investigate the adsorption kinetics of CO_2 on adsorbent using two parameters of DM, the breakthrough curves of CO_2 were measured according to changes of the experimental variables such as flow rate (Q_o) of gaseous mixture of CO_2 and N_2, concentration (C_{Ao}) of CO_2, and adsorption temperature (T).

1. Effect of Flow Rate of Gaseous Mixtures

To study the effect of Q_o on the kinetics, the breakthrough curves of CO_2 were measured according to the change of Q_o from 40-100 cm^3/min (measured at 25 °C) under the typical conditions of C_{Ao} of 5000 ppmv and T of 40 °C. The measured outlet concentrations of CO_2 were plotted against the adsorption time for each flow rate in Fig. 3.

As shown in Fig. 3, a shift of breakthrough curves to shorter times was observed at greater flow rate of the gaseous mixture with decrease in the amount of CO_2 that the bed can hold up to a certain breakthrough level. This result means that the adsorbed amount of CO_2 decreases as the space time of the gaseous mixtures in the fixed bed decreases. The breakthrough curve was evaluated by analysis of the experimental breakthrough data using a nonlinear least squares technique with the parameters of $k_o\tau$ and k_d, from which k_o was obtained. These values are in Table 2. The calculated breakthrough curve (solid line) of CO_2 with the mean values of $k_o\tau$ and k_d is shown

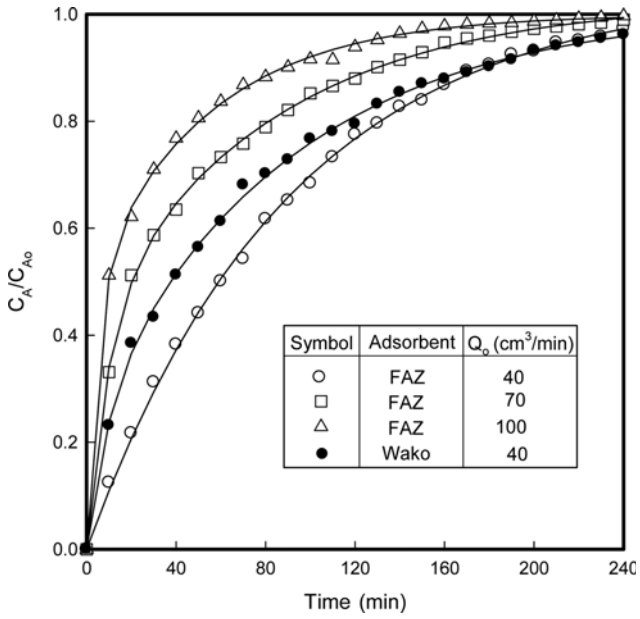

Fig. 3. Effect of flow rates of gaseous mixtures on the breakthrough curve of CO_2 (C_{Ao}=5000 ppmv; T=40 °C).

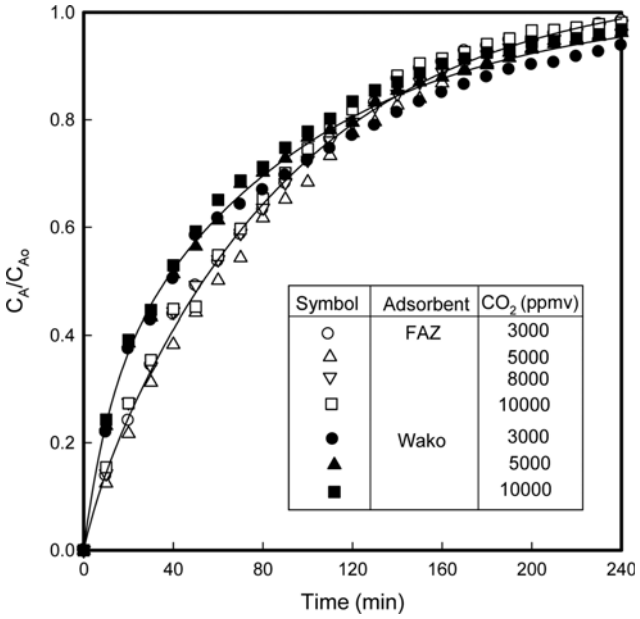

Fig. 4. Breakthrough curves of CO_2 for various feedstock concentrations of CO_2 (Q_o=40 cm³/min; T=40 °C).

in Fig. 3. As shown, the regression analysis of the experimental breakthrough data gave very good agreement with the breakthrough equation, Eq. (4), with regression coefficient (r^2) more than 0.998. As shown in Table 2, the values of $k_o\tau$ decreased with increasing Q_o where the k_o's and k_d's were almost same. This means that the kinetics was independent of the flow rate of gaseous mixture. On the other hand, the breakthrough curve of CO_2 using Wako at Q_o of 40 cm³/min is presented in Fig. 3. Its breakthrough curve shifts to shorter times than FAZ, which makes the fractional adsorbed amount (as mentioned later) smaller than FAZ. The kinetics of Wako is listed in Table 2. The effects of Q_o on the kinetics were similar to FAZ.

2. Effect of Concentration of CO_2

To determine the dependence of the adsorption parameters on the feedstock concentration of CO_2, the breakthrough curves of CO_2

Table 2. Rate parameters at various experimental conditions of FAZ and Wako

Adsorbent	T (°C)	Q_o (cm³/min)	CO_2 (ppmv)	$k_o\times10^7$ (m/min)	$k_o\tau$	k_d (1/min)	r^2	q_f	q (mg/g)
FAZ	40	20	5000	2.19	2.503	0.020	0.9995	0.704	16.51
FAZ	40	40	5000	2.23	1.274	0.018	0.9993	0.532	24.97
FAZ	40	70	5000	2.22	0.725	0.018	0.9995	0.445	36.52
FAZ	40	100	5000	2.20	0.503	0.020	0.9990	0.403	47.28
Wako	40	20	5000	2.23	1.623	0.013	0.9896	0.664	15.57
Wako	40	40	5000	2.21	0.804	0.014	0.9992	0.487	22.86
Wako	40	100	5000	2.22	0.323	0.012	0.9995	0.404	47.34
FAZ	40	40	3000	2.23	1.274	0.020	0.9996	0.514	14.47
FAZ	40	40	5000	2.23	1.274	0.018	0.9993	0.532	24.97
FAZ	40	40	8000	2.17	1.240	0.019	0.9995	0.517	38.85
FAZ	40	40	10000	2.24	1.280	0.021	0.9989	0.507	47.57
Wako	40	40	3000	2.19	0.797	0.012	0.9993	0.505	14.23
Wako	40	40	5000	2.21	0.804	0.014	0.9992	0.487	22.86
Wako	40	40	10000	2.20	0.800	0.015	0.9989	0.478	44.86
FAZ	20	40	5000	1.83	1.117	0.011	0.9996	0.589	25.87
FAZ	40	40	5000	2.23	1.274	0.018	0.9993	0.532	24.97
FAZ	60	40	5000	2.45	1.316	0.029	0.9991	0.464	23.18
FAZ	80	40	5000	2.97	1.505	0.050	0.9995	0.421	22.29
Wako	20	40	5000	1.93	0.750	0.008	0.9994	0.545	23.92
Wako	40	40	5000	2.21	0.804	0.014	0.9992	0.487	22.86
Wako	60	40	5000	2.45	0.838	0.027	0.9989	0.421	21.02
Wako	80	40	5000	2.95	0.920	0.046	0.9991	0.390	20.65

were measured in the range of C_{Ao} from 3000-10000 ppmv under the typical conditions of Q_o of 40 cm^3/min and T of 40 °C. The measured outlet concentrations of CO_2 were plotted for 3000 and 10000 ppmv, respectively, in Fig. 4.

A good fitting of DM predictions to experimental data can be seen by inserting the corresponding values of $k_o\tau$ and k_d provided in Table 2 into Eq. (4). The calculated breakthrough curve (solid line) of CO_2 with the mean values of $k_o\tau$ and k_d and measured ones (various symbols) is shown in Fig. 4. The measured values approach the calculated value with r^2 more than 0.998. This result comes from independence of the concentration of CO_2 on the breakthrough curves as shown in Eq. (4). These results were exhibited equally for other concentrations of CO_2. The breakthrough curves of CO_2 for Wako are presented in Fig. 4 and their CO_2 tendency was as same as that for FAZ.

3. Effect of Adsorption Temperature

To investigate the effect of adsorption temperature on the adsorption kinetics, the breakthrough curves of CO_2 were measured from 20-80 °C under the typical conditions of Q_o of 40 cm^3/min and C_{Ao} of 5000 ppmv. Fig. 5 shows the plots of the measured outlet concentrations of CO_2 vs. the adsorption time.

The results in Fig. 5 indicate a shift in breakthrough curves toward the left with increased temperature, which might be attributed to a decrease in the amount of adsorbed CO_2 due to increase of adsorption and deactivation and was the same result of the breakthrough curves of CO_2 on mesoporous adsorbent of EDA-CP-MS41 [30]. The breakthrough curve of CO_2 for Wako at a typical temperature of 40 °C is presented in Fig. 5 and its breakthrough curve shifts to shorter times than FAZ. The model parameters of both adsorbents were evaluated and tabulated in Table 2.

The Arrhenius plots of k_o and k_d for adsorbents of FAZ and Wako, respectively, are shown in Fig. 6.

The activation energy for the adsorption (ΔE_o) and deactivation (ΔE_d) was obtained from the slopes of plots in Fig. 6, and their values

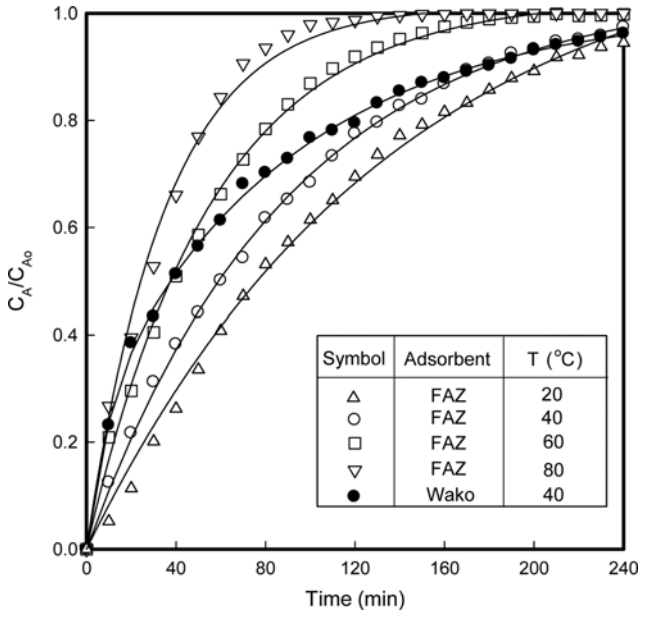

Fig. 5. Breakthrough curves of CO_2 for various adsorption temperatures (Q_o=40 cm^3/min; C_{Ao}=5000 ppmv).

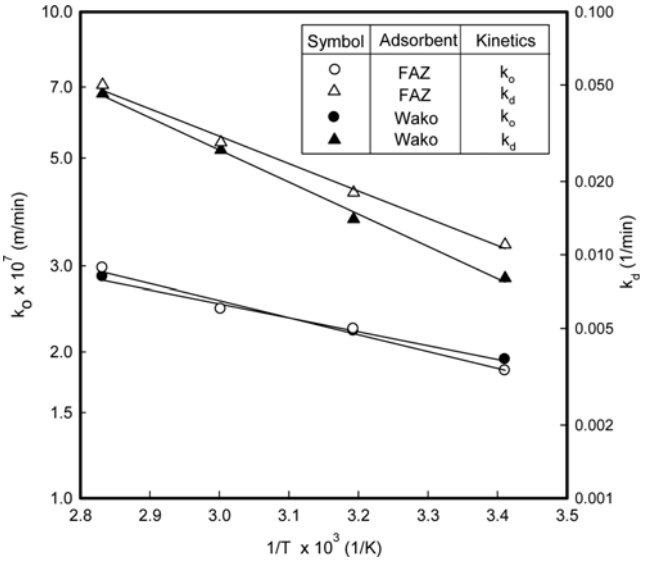

Fig. 6. Effect of temperature on adsorption rate constant and deactivation rate constant for FAZ and Wako (Q_o=40 cm^3/min; C_{Ao}=5000 ppmv).

were 6.64 and 21.51 kJ/mol for FAZ, and 5.45 and 25.34 kJ/mol for Wako, respectively. Linear regression analysis of the Arrhenius plots leads to the following empirical expression for k_o and k_d for FAZ;

$$k_o = 2.80\times10^{-6}\ \mathrm{Exp}(-799/T) \tag{5}$$

$$k_d = 72.3\times\mathrm{Exp}(-2586/T) \tag{6}$$

And, for Wako,

$$k_o = 1.80\times10^{-6}\ \mathrm{Exp}(-656/T) \tag{7}$$

$$k_d = 253\ \mathrm{Exp}(-3048/T) \tag{8}$$

4. Adsorptive Capacity of Adsorbent

The adsorbed amount (q) of CO_2 during an adsorption time (t_f) was obtained by using the breakthrough curve as follows [10]:

$$q = q_o q_f \tag{9}$$

$$q_o = \frac{C_{Ao}Q_oM_wt_f}{W_o} \tag{10}$$

$$q_f = 1 - \frac{1}{t_f}\int_0^{t_f} a(t)dt \tag{11}$$

where q_o is the total inlet amount of the adsorbate, which is dependent on the experimental conditions of C_{Ao}, Q_o, W_o, and t_f, on the other hand, q_f is the fractional amount of adsorption, which is dependent on the physicochemical properties of k_o and k_d.

To observe the adsorptive capacity of an adsorbent, it may be more reasonable and convenient to use q_f rather than q_o, because the expression of the dimensionless group, such as dimensionless rate of adsorption constant ($k_o\tau$) and dimensionless rate of deactivation constant (k_dt_f), can generalize the experimental variables of C_{Ao}, Q_o, and W_o. Because the second term in the right side of Eq. (11) is a portion of unadsorbed amount, q_f is estimated from Eq. (11) with Eq. (4). The values of q_f using the numerical integration of the Simpson rule are plotted vs. $k_o\tau$ with a parameters of k_dt_f in Fig. 7.

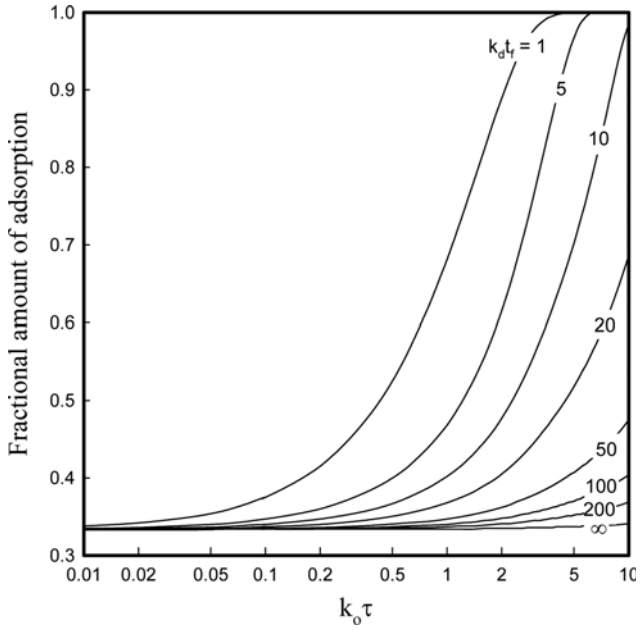

Fig. 7. Fractional amount of adsorption based on Eq. (4) and (11).

As shown in Fig. 7, q_f increased with increasing $k_o\tau$ and decreasing k_dt_f, and approached to an asymptote.

The values of q and q_f, obtained from Eqs. (9) and (11) using the experimental variables of FAZ and Wako, are listed in Table 2. As shown, q_f increased with decreasing Q_o and T, and was independent on the feed concentration of CO_2. These results can be explained by the increase of the upper area of the breakthrough curve due to a shift in breakthrough curves toward the right with decreased Q_o and T, as shown in Figs. 3 and 5. Although k_o's of Wako were larger than those of FAZ, q_f's of Wako were smaller than those of FAZ. This result may be due to larger k_d's of Wako than those of FAZ. To compare q_f between FAZ and Wako, it is proper to use the adsorptive activity rather than k_o and k_d, because the activity is combined with k_o and k_d. The values of α were obtained from Eq. (3) and plotted against the dimensionless adsorption time under the typical conditions, such as Q_o of 40 cm^3/min, C_{Ao} of 5000 ppmv, and T of 40 °C in Fig. 8.

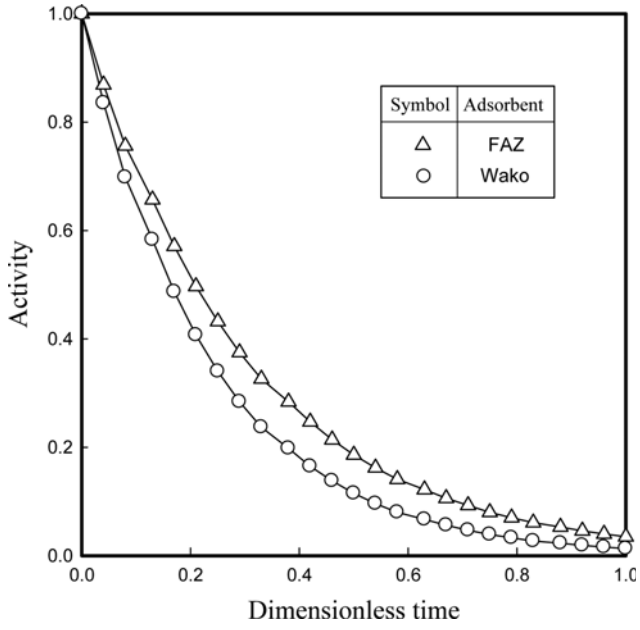

Fig. 8. Activity of the adsorbents (Q_o=40 cm^3/min; T=40 °C; C_{Ao}= 5000 ppmv).

As shown in Fig. 8, the activities of FAZ were larger than them of Wako. These results are exhibited equally for other experimental conditions. This means that the larger the adsorptive activity, the larger the adsorptive capacity. There were little differences of the adsorbed amount of CO_2 between the two adsorbents, as shown in Table 2.

5. Comparison of the Proposed Models of Adsorption Isotherm

Several equilibrium models [21], which have been developed to describe adsorption isotherm relationships, are useful for describing adsorption capacity and some are useful for theoretical evaluation of thermodynamic parameter, such as heats of adsorption. But, the experimental procedure to prepare the adsorption isotherm is very tedious and takes too much time. On the other hand, the equilibrium concentrations between two phases, which are used to describe adsorption isotherm relationships, can be obtained by the following equations of Eqs. (12) and (13), where a(t), x and y are the dimensionless concentrations of CO_2 in the breakthrough data, in the gas phase and solid phase, respectively. The equilibriums for single-solute adsorption given in the literature [9] are frequently presented as dimensionless concentration isotherms.

$$x = \frac{\int_0^t a(t)dt}{\int_0^\infty a(t)dt} \tag{12}$$

$$y = \frac{t - \int_0^t a(t)dt}{\int_0^\infty dt - \int_0^\infty a(t)dt} \tag{13}$$

where, t is the adsorption time and a(t) comes from the breakthrough data or Eq. (4). As shown in Eqs. (12) and (13), the ranges of x and y are between 0 and 1, respectively. The equilibrium isotherm models such as Langmuir, Freundlich, Brunauer-Emmett-Teller (BET), and Dubinin-Radushkevich-Kagener (DRK) model, selected by Suyadal et al. [23], were used to compare with the deactivation model, and their formulas are listed in Table 3.

The values of x and y were obtained from Eqs. (12) and (13) and fitted with the models mentioned above to give the equilibrium isotherm constants (listed in Table 3) of a and b in each model. Under the typical conditions such as Q_o of 40 cm^3/min, C_{Ao} of 5000 ppmv, and T of 40 °C, they were plotted in Fig. 9 as solid lines for each model and as circles for the experimental breakthrough data.

As shown in Table 3 and Fig. 9, the proposed deactivation model fitted the data with r^2 of 0.9993, and FAZ might be favorable for the adsorption of CO_2 due to the separation factor of less than unity. Failure of BET, DRK, Langmuir, and Freundlich models in order in the fitting with the experimental data in Fig. 9 may be explained by the gas-solid heterogeneous reaction containing adsorption between CO_2 and FAZ. BET model is an extended model of Langmuir model and includes multi-layer adsorption phenomena. The BET has as-

Table 3. Selected adsorption isotherms to fit the breakthrough data of CO_2 for comparison with the deactivation model (Q_o=40 cm^3/min; T=40 °C; C_{Ao}=5000 ppmv)

Adsorption isotherms	Mathematical representation of adsorption isotherms	Linearized forms	Parameters and correlation coefficient
Langmuir	$y=\frac{ax}{1+bx}$	$\frac{1}{y}=\frac{1}{ax}+\frac{b}{a}$	a=3.8446 b=3.3154 r^2=0.8562
Freundlich	$y=ax^b$	$\ln(y)=\ln(a)+b\ln(x)$	a=1.1120 b=0.6360 r^2=0.9842
Brunauer-Emmett-Teller	$y=\frac{x}{(1-x)(a+bx)}$	$\frac{x}{y(1-x)}=a+bx$	a=1.5079 b=9.4222 r^2=0.7288
Dubinin-Radshkevich-Kagener	$y=a\exp[-b\ln^2(x)]$	$\ln(y)=\ln(a)-b\ln^2(x)$	a=0.7975 b=0.1696 r^2=0.7562
Deactivation model (this study)	x according to Eq. (12) y according to Eq. (13)		$k_o\tau$=1.274 k_d=0.0180 r^2=0.9913

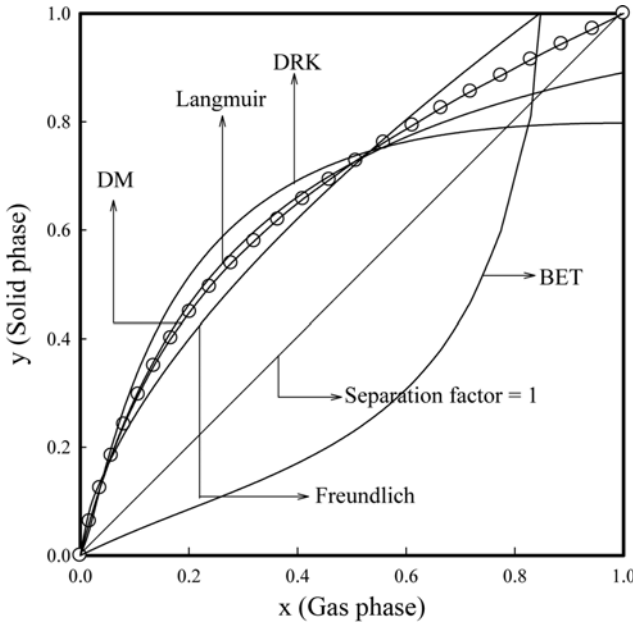

Fig. 9. Comparison of the model of adsorption isotherm in describing the experimental breakthrough curve of CO_2 according to Table 3 (Q_o=40 cm^3/min; T=40 °C; C_{Ao}=5000 ppmv).

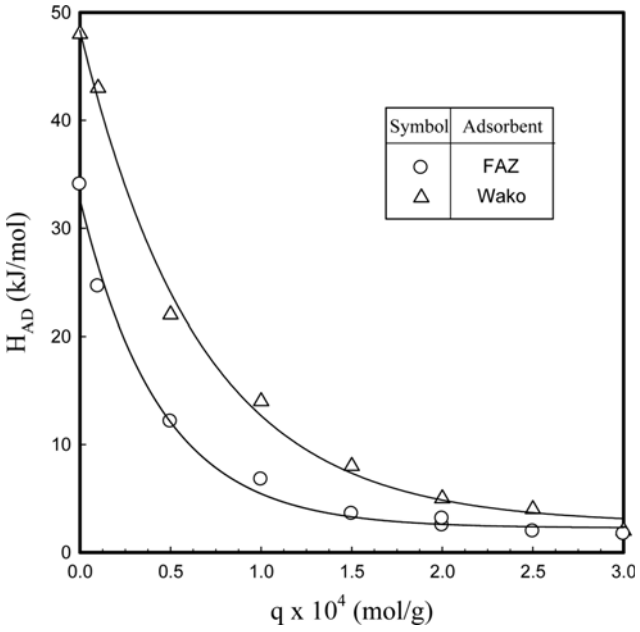

Fig. 10. Isosteric heat of adsorption for CO_2 on adsorbent at 40 °C.

sumptions that any given layer need not be completed before subsequent layers can form, that the first layer of molecules adheres to the surface with a comparable energy to the heat of adsorption for monolayer attachment, and that subsequent layers are essentially condensation reactions [12]. As shown in Fig. 9, the BET model was not fitted with the experimental data. From this result, the practical adsorption situation in this study may not be the multi-layer adsorption phenomenon.

6. Heat of Adsorption

When an adsorbent adsorbs one or more adsorbates, adsorption heat is usually generated since all adsorption processes are exothermic. Eventually, the evolved affects the adsorption performance considerably. If the adsorption system was very ideal following the Langmuir isotherm, the heat of adsorption would be independent of the amount adsorbed. However, it would not be true for most adsorption processes because of the energetically heterogeneous surfaces of adsorbents. The isosteric heat of adsorption (H_{AD}) may be evaluated simply by applying the modified Clausius-Clapeyron equation [39] if one has a good set of adsorption equilibrium data obtained at several temperatures as follows:

$$\frac{H_{AD}}{RT^2}=\frac{\partial\ln(x)}{\partial T} \tag{14}$$

As shown in Table 3, the adsorption isotherms are equivalent to the

relationship between x and y of Eqs. (12) and (13), and then, x is substituted for p/p_o in the Clausius-Clapeyron equation. H_{AD} was estimated from the slope of plots of ln(x) vs. temperature using parameter of q. H_{AD} for FAZ and Wako are shown in Fig. 10 under the typical conditions, such as Q_o of 40 cm^3/min, C_{Ao} of 5000 ppmv, and T of 40 °C. As shown in Fig. 10, the H_{AD} of Wako was larger than them of FAZ, but the differences between them were small.

CONCLUSIONS

Zeolite was synthesized by the fusion method using coal fly ash to capture carbon dioxide, and the breakthrough data were measured in a fixed bed to obtain the adsorption kinetics. The deactivation model was used to evaluate the adsorption kinetics based on the adsorption rate constant and deactivation rate constant by fitting the experimental breakthrough data with the model using a nonlinear least squares technique. The adsorption kinetics was assumed to be the first-order with respect to the concentration of carbon dioxide and the activity of the adsorbent, respectively. The experimental breakthrough data fitted very well to the deactivation model than the adsorption isotherm models in the literature, and could be used for preparation of the adsorbed amount and heat of adsorption. The adsorptive activity and capacity of FAZ were larger than those of the commercial zeolite of Wako 4A. There was little difference in the adsorbed amount of CO_2 between the two adsorbents, the use of a commercial zeolite such as silicate was not cost-effective, and FAZ could be synthesized from coal fly ash as a reuse of the wastes.

NOMENCLATURE

a : C_A/C_{Ao}
C_A : concentration of CO_2 [kmol/m^3]
C_{Ao} : inlet concentration of CO_2 in gas phase [kmol/m^3] or [ppmv]
k_o : adsorption rate constant [m/min]
k_d : deactivation rate constant [1/min]
m : reaction order with respect to α
M_w : molecular weight of adsorbate [kg/kmol]
n : reaction order with respect to C_A
q : adsorbed amount of adsorbate [mg/g] or [mol/kg]
q_f : fraction of adsorbed amount defined as q/q_o
q_o : total inlet amount of the adsorbate [mg/g] or [mol/kg]
Q_o : volumetric flow rate of gaseous mixture [cm^3/min]
R : gas law constant 8.314 [J/mol·K]
r^2 : correlation coefficient
S : vacant surface area of the adsorbent [m^2]
S_o : specific initial vacant surface area of the adsorbent [m^2/kg]
t : adsorption time [min]
t_f : operational adsorption time [min]
T : adsorption temperature [°C]
W_o : feed amount of the adsorbent [kg]
x : dimensionless concentrations of CO_2 in the gas phase through adsorption isotherm
y : dimensionless concentrations of CO_2 in the solid phase through adsorption isotherm

Greek Letters

α : activity of the adsorbent
τ : surface time defined as W_oS_o/Q_o [min/m]

Subscripts

A : CO_2

REFERENCES

1. M. Aresta, *Carbon dioxide recovery and utilization*, Kluwer Academic Pub., Boston (2003).
2. R. K. Bartoo, *Chem. Eng. Prog*., **80**, 35 (1984).
3. T. D. Pham, Q. Liu and R. F. Lobo, *Langmuir*, **29**, 832 (2013).
4. G. Aguilar-Armenta, G. Hernandez-Ramirez, E. Flores-Loyola, A. Ugarte-Castaneda, R.Silva-Gonzalez, C. Tabares-Munoz, A. Jimenez-Lopez and E. Rodriguez-Castellon, *J. Phys. Chem.*, **105**, 1313 (2001).
5. J. Kim, L. C. Lin, J. A. Swisher, M. Haranczyk and B. Smit, *J. Am. Chem. Soc*., **134**, 18940 (2012).
6. R. V. Siriwardane, M. S. Shen and E. P. Fisher, *Energy Fuel*, **17**, 571 (2003).
7. J. Shang, G. Li, R. Singh, Q. Gu, K. M. Nairn, T. J. Bastow, N. Medhekar, C. M. Doherty, A. J. Hill, J. Z. Liu and P. A. Webley, *J. Am. Chem. Soc*., **134**, 19246 (2012).
8. V. Kumar, N. Labhsetwar, S. Meshram and S. Rayalu, *Energy Fuel*, **25**, 4854 (2011).
9. S. T. Yang, J. Kim and W. S. Ahn, *Micropor. Mesopor. Mater.*, **135**, 90 (2010).
10. S. Saha, S. Chandra, B. Garai and R. Banerjee, *Indian J. Chem.*, **51A**, 1223 (2012).
11. J. S. Lee, J. H. Kim, J. T. Kim, J. K. Suh, J. M. Lee and C. H. Lee, *J. Chem. Eng. Data*, **47**, 1237 (2002).
12. D. Ferreira, R. Magalhaes, P. Taveira and A. Mendes, *I&EC Research*, **50**, 10201 (2011).
13. M. R. Hudson, W. L. Queen, J. A. Mason, D. W. Fickel, R. F. Lobo and C. M. Brown, *J. Am. Chem. Soc*., **134**, 1970 (2012).
14. T. C. Golden and S. Sircar, *J. Colloid Interface Sci*., **162**, 182 (1994).
15. H. Tanaka, H. Eguchi, S. Fujimoto and R. Hino, *Fuel*, **85**, 1329 (2006).
16. K. Ojha, N. C. Pradhan and A. N. Samanta, *Bull. Mater*., **B77**, 555 (2004).
17. A. Srinivasan and M. W. Grutzeck, *Environ. Sci. Technol*., **33**, 1464 (1999).
18. R. T. Yang, *Gas separation by adsorption processes*, Butterworth, Boston (1987).
19. L. K. Doraiswamy and M. M. Sharma, *Heterogeneous reactions*, Wiley, New York (1984).
20. N. Orbey, G. Dogu and T. Dogu, *Can. J. Chem. Eng*., **60**, 314 (1982).
21. M. Suzuki, *Adsorption engineering*, Kodansga Ltd., Tokyo (1990).
22. S. Yasyerli, T. Dogu, G. Dogu and I. Ar, *Chem. Eng. Sci*., **51**, 2523 (1996).
23. Y. Suyadal, M. Erol and M. Oguz, *Ind. Eng. Chem. Res.*, **39**, 724 (2000).
24. T. Kopac and S. Kocabas, *Chem. Eng. Commun*., **190**, 1041 (2003).
25. S. W. Park, D. H. Sung, B. S. Choi, K. W. Oh and K. H. Moon, *Sep. Sci. Technol*., **41**, 2665 (2006).
26. S. W. Park, D. H. Sung, B. S. Choi, J. W. Lee and H. Kumazawa, *J. Ind. Eng. Chem.*, **12**, 522 (2006).
27. K. S. Hwang, S. W. Park, D. W. Park, K. W. Oh and S. S. Kim,

Korean J. Chem. Eng., **26**, 1383 (2009).
28. S. W. Park, B. S. Choi and J. W. Lee, *Sep. Sci. Technol*., **42**, 2221 (2007).
29. K. J. Oh, D. W. Park, S. S. Kim and S. W. Park, *Korean J. Chem. Eng*., **27**, 632 (2010).
30. K. S. Hwang, Y. S. Son, S. W. Park, D. W. Park, K. J. Oh and S. S. Kim, *Sep. Sci. Technol*., **45**, 85 (2010).
31. K. S. Hwang, L. Han, D. W. Park, K. J. Oh, S. S. Kim and S. W. Park, *Korean J. Chem. Eng*., **27**, 241 (2010).
32. Y. S. Choe, K. J. Oh, S. S. Kim and S. W. Park, *Korean J. Chem. Eng*., **27**, 962 (2010).
33. T. Kopac and S. Kocabas, *Chem. Eng. Commun*., **190**, 1041 (2003).
34. T. Dogu, *Am. Inst. Chem. Eng. J*., **32**, 849 (1986).
35. J. LaRosa, S. Hwan and M. W. Grutzeck, *J. Am. Ceram. Soc*., **75**, 1574 (1992).
36. X. Querol, N. Moreno, J. C. Umaña, A. Alastuey, E. Hernández, A. Lopez-Sóler and F. Plana, *Int. J. Coal Geology*, **50**, 413 (2002).
37. N. Murayama, H. Yamamoto and J. Shibata, *Int. J. Min. Process*, **64**, 1 (2004).
38. A. Molina and C. Poole, *Min. Eng*., **17**, 167 (2004).
39. D. Kim, W. G. Shim and H. Moon, *Korean J. Chem. Eng*., **18**, 518 (2001).